

Modeling the odds of malignancy for a breast mass using Bayesian logistic regression

Lowell Monis^{*,†}

Abstract. This report presents a Bayesian approach to classifying breast cancer diagnoses (malignant vs. benign) using 30 features computed from a digitized image of a fine needle aspirate of breast masses. Bayesian logistic regression is employed with Metropolis-Hastings sampling for inference. Bayesian variable selection is implemented to identify the most important diagnostic features.

1 Introduction

2 Breast cancer remains one of the most prevalent
3 and life-threatening diseases worldwide. Early
4 and accurate diagnosis is crucial for effective
5 treatment and improved patient outcomes. Fine
6 needle aspiration (FNA) is a minimally invasive
7 diagnostic procedure that extracts cells from a
8 breast mass for analysis. The advent of digital
9 imaging technology has enabled the extraction
10 of quantitative features from these cell nuclei,
11 opening new avenues for automated diagnosis
12 using statistical and machine learning methods.

13 The Wisconsin Diagnostic Breast Cancer
14 (WDBC) dataset, curated by [Wolberg et al.](#)
15 (1993) at the University of Wisconsin, repre-
16 sents a landmark contribution to this field. The
17 dataset contains measurements computed from
18 digitized images of fine needle aspirates, captur-
19 ing various characteristics of cell nuclei that dis-
20 tinguish malignant from benign breast masses.
21 Previous research has demonstrated that these
22 features contain sufficient information to achieve
23 highly accurate classification, with some studies
24 reporting predictive accuracy exceeding 97% us-
25 ing linear programming-based methods.

26 While classical machine learning approaches
27 have proven effective, they often provide point
28 estimates without quantifying the uncertainty
29 in predictions or model parameters. Bayesian
30 methods offer a principled framework for in-
31 corporating prior knowledge, quantifying uncer-
32 tainty, and performing model selection in a prob-
33 abilistic manner. In this analysis, a Bayesian lo-

34 gistic regression approach is adopted to model
35 the probability of malignancy as a function of
36 the extracted features. This approach not only
37 provides predictions but also yields posterior in-
38 formation for all model parameters, enabling
39 greater understanding of the effect of each in-
40 dividual quantifier and the role it plays in the
41 malignancy of a breast mass when prior infor-
42 mation is provided to the model.

43 Objectives

44 This study addresses the following question:

45 Can an accurate Bayesian logistic
46 regression model be developed to
47 predict a breast cancer diagnosis
48 from digitized cell nuclei features,
49 and which of the thirty morpholog-
50 ical characteristics are most predic-
51 tive of malignancy and should be
52 prioritized in clinical diagnosis?

53 Specifically, this study will:

- 54 • Build a Bayesian logistic regression model
55 using all 30 available features and assess its
56 predictive accuracy
- 57 • Quantify the importance of each feature
58 through posterior probabilities
- 59 • Compare the Bayesian variable selection
60 results with classical model selection ap-
61 proaches (AIC/BIC)

62 **The Data**

63 The Wisconsin Diagnostic Breast Cancer
 64 dataset was collected at the University of
 65 Wisconsin Clinical Sciences Center starting
 66 around 1989. It contains measurements from
 67 569 patients who underwent fine needle aspi-
 68 ration of breast masses. For each patient, a
 69 digitized image of the aspirate was analyzed
 70 to compute quantitative features describing
 71 the characteristics of cell nuclei present in the
 72 image. The first feature, `id`, identifies each
 73 sample in the dataset. This feature can be
 74 discarded since it cannot be used as a predictor
 75 variable in the analysis.

```

76 ## 'data.frame': 569 obs. of 32 variables:
77 ## $ id : int 842302 842...
78 ## $ diagnosis : chr "M" "M" ...
79 ## $ radius1 : num 18 20.6 19...
80 ## $ texture1 : num 10.4 17.8 ...
81 ## $ perimeter1 : num 122.8 132...116
82 ## $ area1 : num 1001 1326 ...
83 ## $ smoothness1 : num 0.1184 0.0...117
84 ## $ compactness1 : num 0.2776 0.0...118
85 ## $ concavity1 : num 0.3001 0.0...119
86 ## $ concave_points1 : num 0.1471 0.0...120
87 ## $ symmetry1 : num 0.242 0.18...
88 ## $ fractal_dimension1: num 0.0787 0.0...121
89 ## $ radius2 : num 1.095 0.54...122
90 ## $ texture2 : num 0.905 0.73...123
91 ## $ perimeter2 : num 8.59 3.4 4...124
92 ## $ area2 : num 153.4 74.1...125
93 ## $ smoothness2 : num 0.0064 0.0...126
94 ## $ compactness2 : num 0.049 0.01...127
95 ## $ concavity2 : num 0.0537 0.0...128
96 ## $ concave_points2 : num 0.0159 0.0...129
97 ## $ symmetry2 : num 0.03 0.013...130
98 ## $ fractal_dimension2: num 0.00619 0...
99 ## $ radius3 : num 25.4 25 23...
100 ## $ texture3 : num 17.3 23.4 ...131
101 ## $ perimeter3 : num 184.6 158...132
102 ## $ area3 : num 2019 1956 ...
103 ## $ smoothness3 : num 0.162 0.12...133
104 ## $ compactness3 : num 0.666 0.18...134
105 ## $ concavity3 : num 0.712 0.24...135
106 ## $ concave_points3 : num 0.265 0.18...136
107 ## $ symmetry3 : num 0.46 0.275...137
108 ## $ fractal_dimension3: num 0.1189 0.0...138

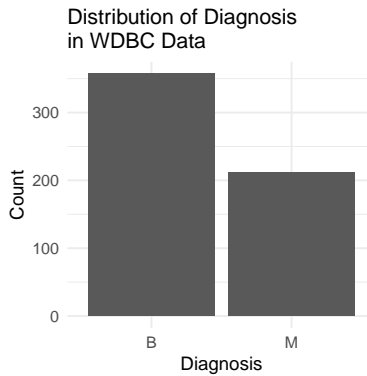
```

109 The dataset contains one binary response
 110 variable where B = benign, and M = malignant.

```

111 ## # A tibble: 2 x 3
112 ## diagnosis count percentage
113 ## <chr>     <int>      <dbl>
114 ## 1 B          357       62.7
115 ## 2 M          212       37.3

```



Apart from the response variable, there are also 30 continuous predictor variables. The 30 real-valued predictor variables are organized into three groups of ten measurements each.

- If the variable ends with 1, these are the mean values averaging each measured value across all cell nuclei in the image.
- If the variable ends with 2, this indicates the standard error of each measured value across all cell nuclei.
- If the variable ends with 3, the feature stores the mean of the three largest (or the worst possible measurements) of each measured value.

The ten base measurements computed for each cell nucleus are:

- *Radius*: Mean distance from center to points on the perimeter.
- *Texture*: Standard deviation of gray-scale values.
- *Perimeter*: Perimeter of the nucleus.
- *Area*: Area of the nucleus.

```

139      • Smoothness: Local variation in radius 188 ## Median :0.3242 Median :1.1080
140      lengths 189 ## Mean :0.4052 Mean :1.2169
141      • Compactness: Computed as perimeter2 / 190 ## 3rd Qu.:0.4789 3rd Qu.:1.4740
142      area - 1.0 191 ## Max. :2.8730 Max. :4.8850
143      • Concavity: Severity of concave portions of 192 ## perimeter2 area2
144      the contour 193 ## Min. : 0.757 Min. : 6.802
145      • Concave points: Number of concave por- 194 ## 1st Qu.: 1.606 1st Qu.: 17.850
146      tions of the contour 195 ## Median : 2.287 Median : 24.530
147      • Symmetry: Symmetry of the nucleus 196 ## Mean : 2.866 Mean : 40.337
148      • Fractal dimension: "Coastline approxima- 197 ## 3rd Qu.: 3.357 3rd Qu.: 45.190
149      tion" - 1 198 ## Max. :21.980 Max. :542.200
199 ## smoothness2 compactness2
150 ## radius1 texture1 200 ## Min. :0.001713 Min. :0.002252
151 ## Min. : 6.981 Min. : 9.71 201 ## 1st Qu.:0.005169 1st Qu.:0.013080
152 ## 1st Qu.:11.700 1st Qu.:16.17 202 ## Median :0.006380 Median :0.020450
153 ## Median :13.370 Median :18.84 203 ## Mean :0.007041 Mean :0.025478
154 ## Mean :14.127 Mean :19.29 204 ## 3rd Qu.:0.008146 3rd Qu.:0.032450
155 ## 3rd Qu.:15.780 3rd Qu.:21.80 205 ## Max. :0.031130 Max. :0.135400
156 ## Max. :28.110 Max. :39.28 206 ## concavity2 concave_points2
157 ## perimeter1 area1 207 ## Min. :0.000000 Min. :0.000000
158 ## Min. : 43.79 Min. : 143.5 208 ## 1st Qu.:0.01509 1st Qu.:0.007638
159 ## 1st Qu.: 75.17 1st Qu.: 420.3 209 ## Median :0.02589 Median :0.010930
160 ## Median : 86.24 Median : 551.1 210 ## Mean :0.03189 Mean :0.011796
161 ## Mean : 91.97 Mean : 654.9 211 ## 3rd Qu.:0.04205 3rd Qu.:0.014710
162 ## 3rd Qu.:104.10 3rd Qu.: 782.7 212 ## Max. :0.39600 Max. :0.052790
163 ## Max. :188.50 Max. :2501.0 213 ## symmetry2 fractal_dimension2
164 ## smoothness1 compactness1 214 ## Min. :0.007882 Min. :0.0008948
165 ## Min. :0.05263 Min. :0.01938 215 ## 1st Qu.:0.015160 1st Qu.:0.0022480
166 ## 1st Qu.:0.08637 1st Qu.:0.06492 216 ## Median :0.018730 Median :0.0031870
167 ## Median :0.09587 Median :0.09263 217 ## Mean :0.020542 Mean :0.0037949
168 ## Mean :0.09636 Mean :0.10434 218 ## 3rd Qu.:0.023480 3rd Qu.:0.0045580
169 ## 3rd Qu.:0.10530 3rd Qu.:0.13040 219 ## Max. :0.078950 Max. :0.0298400
170 ## Max. :0.16340 Max. :0.34540 220 ## radius3 texture3
171 ## concavity1 concave_points1 221 ## Min. : 7.93 Min. :12.02
172 ## Min. :0.000000 Min. :0.000000 222 ## 1st Qu.:13.01 1st Qu.:21.08
173 ## 1st Qu.:0.02956 1st Qu.:0.02031 223 ## Median :14.97 Median :25.41
174 ## Median :0.06154 Median :0.03350 224 ## Mean :16.27 Mean :25.68
175 ## Mean :0.08880 Mean :0.04892 225 ## 3rd Qu.:18.79 3rd Qu.:29.72
176 ## 3rd Qu.:0.13070 3rd Qu.:0.07400 226 ## Max. :36.04 Max. :49.54
177 ## Max. :0.42680 Max. :0.20120 227 ## perimeter3 area3
178 ## symmetry1 fractal_dimension1 228 ## Min. : 50.41 Min. : 185.2
179 ## Min. :0.1060 Min. :0.04996 229 ## 1st Qu.: 84.11 1st Qu.: 515.3
180 ## 1st Qu.:0.1619 1st Qu.:0.05770 230 ## Median : 97.66 Median : 686.5
181 ## Median :0.1792 Median :0.06154 231 ## Mean :107.26 Mean : 880.6
182 ## Mean :0.1812 Mean :0.06280 232 ## 3rd Qu.:125.40 3rd Qu.:1084.0
183 ## 3rd Qu.:0.1957 3rd Qu.:0.06612 233 ## Max. :251.20 Max. :4254.0
184 ## Max. :0.3040 Max. :0.09744 234 ## smoothness3 compactness3
185 ## radius2 texture2 235 ## Min. :0.07117 Min. :0.02729
186 ## Min. :0.1115 Min. :0.3602 236 ## 1st Qu.:0.11660 1st Qu.:0.14720
187 ## 1st Qu.:0.2324 1st Qu.:0.8339 237 ## Median :0.13130 Median :0.21190

```

```

238 ## Mean    :0.13237   Mean    :0.25427
239 ## 3rd Qu.:0.14600   3rd Qu.:0.33910
240 ## Max.    :0.22260   Max.    :1.05800
241 ## concavity3      concave_points3
242 ## Min.    :0.00000   Min.    :0.00000
243 ## 1st Qu.:0.1145   1st Qu.:0.06493
244 ## Median :0.2267   Median :0.09993
245 ## Mean    :0.2722   Mean    :0.11461
246 ## 3rd Qu.:0.3829   3rd Qu.:0.16140
247 ## Max.    :1.2520   Max.    :0.29100
248 ## symmetry3       fractal_dimension3
249 ## Min.    :0.1565   Min.    :0.05504
250 ## 1st Qu.:0.2504   1st Qu.:0.07146
251 ## Median :0.2822   Median :0.08004
252 ## Mean    :0.2901   Mean    :0.08395
253 ## 3rd Qu.:0.3179   3rd Qu.:0.09208
254 ## Max.    :0.6638   Max.    :0.20750

```

255 All feature values were recorded with four
 256 significant digits, and the dataset contains no
 257 missing values according to its description. Pre-
 258 vious research has shown that these 30 fea-
 259 tures contain sufficient information to achieve
 260 linear separability of the two diagnostic classes,
 261 with particularly strong predictive power coming
 262 from features such as worst area, worst smooth-
 263 ness, and mean texture.

278 as follows:

$$\mathbf{X} = \begin{bmatrix} 1 & x_{1,1} & x_{1,2} & \cdots & x_{1,30} \\ 1 & x_{2,1} & x_{2,2} & \cdots & x_{2,30} \\ \vdots & \vdots & \vdots & \ddots & \vdots \\ 1 & x_{n,1} & x_{n,2} & \cdots & x_{n,30} \end{bmatrix}_{n \times p}$$

279 where $n = 569$ patients, $p = 31$ parameters
 280 (1 intercept + 30 features), and $x_{i,j}$ represents
 281 the value of feature j for patient i .

282 To do this, the features are bound with an
 283 all-ones vector column-wise:

$$\mathbf{X} = [\mathbf{1}_n \mid \mathbf{X}_{\text{features}}] \in \mathbb{R}^{n \times p}$$

284 Following through the observations made
 285 earlier about the difference in the scales of each
 286 feature, the design matrix can be standardized
 287 to $\mathcal{N}(0, 1)$ to improve the performance of algo-
 288 rithms like Metropolis-Hastings, and make the
 289 interpretation of coefficients more meaningful.

$$\mathbf{X}_{\text{scaled}} = \frac{\mathbf{X} - \mu}{\sigma}$$

264 Preprocessing

290 Model Setup

291 The first, and most important preprocessing step
 292 while preparing the data for analysis is to encode
 293 the response variable into something more ac-
 294 ceptable to a numerical model. Since this model
 295 aims to predict malignancy in a breast mass, a
 296 response that the mass is malignant is set to 1,
 297 while a response that the mass is benign is set
 298 to 0.

$$y = \begin{cases} 0, & \text{mass is benign} \\ 1, & \text{mass is malignant} \end{cases}$$

299 Since the response variable for this analysis is bi-
 300 nary (malignant or benign), a logistic regression
 301 model is the appropriate choice for classification.
 302 The goal is to estimate the probability that a
 303 breast mass is malignant given the observed fea-
 304 ture measurements. A Bayesian approach will be
 305 employed to quantify uncertainty in both predic-
 306 tions and parameter estimates.

299 For each observation $i = 1, \dots, n$, where $n =$
 300 569 patients, the response variable Y_i follows a
 301 Bernoulli distribution:

$$Y_i \mid \mathbf{x}_i, \beta \sim \text{Bernoulli}(\theta_i)$$

302 Here $Y_i \in \{0, 1\}$ indicates whether patient i has
 303 a malignant or benign mass. \mathbf{x}_i is the vector of
 304 30 feature measurements for patient i (and an in-
 305 tercept value), and $\beta = (\beta_0, \beta_1, \dots, \beta_{30})^T$ is the
 306 vector of regression coefficients to be estimated,

```

273 ##
274 ## y      B    M
275 ## 0 357  0
276 ## 1 0 212

```

277 The design matrix needs to be constructed

307 containing the intercept and 30 coefficients cor- 334
 308 responding to each feature, which quantify the 335
 309 effect of each measurement on the odds of malig- 336
 310 nancy. The probability of malignancy for patient 337
 311 i is modeled:

$$\theta_i = P(Y_i = 1 \mid \mathbf{x}_i, \boldsymbol{\beta}) = \frac{e^{\boldsymbol{\beta}^T \mathbf{x}_i}}{1 + e^{\boldsymbol{\beta}^T \mathbf{x}_i}}$$

312 This function, known as the logistic or sigmoid 338
 313 function, ensures that predicted probabilities lie 339
 314 between 0 and 1, making it suitable for binary 340
 315 classification problems.

316 Equivalently, this can also be expressed us- 341
 317 ing its logit transformation as follows:

$$\begin{aligned}\text{logit}(\theta_i) &= \log\left(\frac{\theta_i}{1 - \theta_i}\right) \\ &= \boldsymbol{\beta}^T \mathbf{x}_i \\ &= \beta_0 + \sum_{j=1}^{30} \beta_j x_{i,j}\end{aligned}$$

318 The left-hand side represents the log-odds of 342
 319 malignancy, which is modeled as a linear combi- 343
 320 nation of the features.

321 The likelihood function quantifies the 344
 322 probability of observing the response $\mathbf{y} = 345$
 $(y_1, y_2, \dots, y_n)^T$ given the feature matrix \mathbf{X} and 346
 323 coefficient vector $\boldsymbol{\beta}$. Under the assumption that 347
 324 observations are independent, the joint likeli- 348
 325 hood is the product of individual Bernoulli prob- 349
 326 abilities:

$$\begin{aligned}p(\mathbf{y} \mid \mathbf{X}, \boldsymbol{\beta}) &= \prod_{i=1}^n \theta_i^{y_i} (1 - \theta_i)^{1-y_i} \\ &= \prod_{i=1}^n \frac{e^{\boldsymbol{\beta}^T \mathbf{x}_i}}{1 + e^{\boldsymbol{\beta}^T \mathbf{x}_i}}\end{aligned}$$

328 The expression follows from the Bernoulli 361
 329 probability mass function—when $y_i = 1$ (ma- 362
 330 lignant), the contribution is θ_i , and when $y_i = 0$ 363
 331 (benign), the contribution is $1 - \theta_i$. The expan- 364
 332 sion of the expression is provided by substituting 365
 333 the logistic function θ_i .

334 For numerical stability and computational 335 efficiency, it is standard practice to work with 336 the log-likelihood. Taking the natural logarithm 337 of both sides and applying the properties of log- 338 arithms, one can obtain:

$$\begin{aligned}\log p(\mathbf{y} \mid \mathbf{X}, \boldsymbol{\beta}) &= \sum_{i=1}^n \log \left[\frac{e^{\boldsymbol{\beta}^T \mathbf{x}_i}}{1 + e^{\boldsymbol{\beta}^T \mathbf{x}_i}} \right] \\ &= \sum_{i=1}^n \left[\log(e^{\boldsymbol{\beta}^T \mathbf{x}_i}) - \log(1 + e^{\boldsymbol{\beta}^T \mathbf{x}_i}) \right] \\ &= \sum_{i=1}^n \left[y_i \boldsymbol{\beta}^T \mathbf{x}_i - \log(1 + e^{\boldsymbol{\beta}^T \mathbf{x}_i}) \right]\end{aligned}$$

339 The log-likelihood form is computationally 340
 341 advantageous due to its ability to convert prod- 342
 343 ucts into sums, which are numerically more 344
 345 stable, and avoid potential underflow issues 346
 347 when multiplying many small probabilities. It 348
 349 is also the foundation for constructing the ac- 350
 351 ceptance ratio in the Metropolis-Hastings algo- 352
 353 rithm, which will be explored later in this study.

347 Prior Distribution

348 In Bayesian inference, prior distributions encode 349
 350 beliefs about parameters before observing the 351
 352 data. For this analysis, a weakly informative 353
 354 multivariate normal prior is adopted for the co- 355
 356 efficient vector $\boldsymbol{\beta}$:

$$\boldsymbol{\beta} \sim \mathcal{N}(\boldsymbol{\mu}_0, \Sigma_0)$$

357 where $\boldsymbol{\mu}_0 = \mathbf{0}_p$, $p = 31$, giving a 31- 358
 359 dimensional all-zeros vector, and $\Sigma_0 = \sigma_0^2 \mathbf{I}_p$, 360
 361 where $\sigma_0^2 = 100$, and \mathbf{I}_p is the 31×31 iden- 362
 363 tity matrix. This choice reflects several impor- 364
 365 tant considerations. First, centering the prior 366
 367 at zero with prior mean set to 0 indicates no 368
 369 prior preference for the direction or magnitude 370
 371 of effects—it is not assumed *a priori* that any 372
 373 feature increases or decreases the probability of 374
 375 malignancy. Second, the large prior variance, set 376
 377 to 100, makes this a weakly informative prior, 378
 379 meaning the data will largely determine the pos- 380
 381 terior estimates, rather than being heavily influ- 382
 383 enced by prior assumptions. The independence

367 structure impose by the diagonal covariance ma-
 368 trix Σ_0 assumes that, prior to seeing the data,
 369 there is no reason to believe the coefficients are
 370 correlated with one another.

371 Despite being weakly informative, this prior
 372 serves an important regularization function by
 373 gently discouraging extremely large coefficient
 374 values that might lead to overfitting or numerical
 375 instability. However, unlike conjugate priors in
 376 simpler models such as the normal-normal model
 377 for linear regression, this prior does not combine
 378 with the logistic likelihood to produce a poste-
 379 rior distribution with a known, closed-form ex-
 380 pression. Consequently, the posterior summaries
 381 cannot be obtained analytically, and computa-
 382 tional methods must be used.

383 Posterior Distribution

384 The posterior distribution combines the likeli-
 385 hood and prior through Bayes' theorem:

403 This is because the logistic likelihood is not con-
 404 jugate to the normal prior. The product of these
 405 two densities does not simplify to a recogniz-
 406 able probability distribution. As a result, pos-
 407 terior means, variances, and credible intervals
 408 cannot be computed using direct integration or
 409 algebraic manipulation.

410 This necessitates the use of Markov Chain
 411 Monte Carlo methods to generate samples from
 412 the posterior distribution. By drawing a large
 413 number of samples $\beta^{(1)}, \beta^{(2)}, \dots, \beta^{(S)}$ from
 414 $p(\beta | \mathbf{y}, \mathbf{X})$ for a total of S simulations, the pos-
 415 terior summaries can be approximated empiri-
 416 cally: posterior means can be estimated by sam-
 417 ple averages, and credible intervals can be con-
 418 structed from sample quantiles. The Metropolis-
 419 Hastings algorithm, described in the following
 420 section, provides the computational framework
 421 for generating these samples. The Gibbs sampler
 422 is not directly applicable, since the full condi-
 423 tional distributions do not have closed-form ex-
 424 pressions either.

$$p(\beta | \mathbf{y}, \mathbf{X}) = \frac{p(\mathbf{y} | \mathbf{X}, \beta) \cdot p(\beta)}{p(\mathbf{y} | \mathbf{X})}$$

425

386 The denominator $p(\mathbf{y} | \mathbf{X}) = \int p(\mathbf{y} |$
 387 $\mathbf{X}, \beta)p(\beta)d\beta$ is the marginal likelihood, which
 388 serves as a normalizing constant ensuring the
 389 posterior integrates to one. Since this integral is
 390 difficult to handle for logistic support, the unnor-
 391 malized posterior is used, which is proportional
 392 to the product of the likelihood and the prior:

$$p(\beta | \mathbf{y}, \mathbf{X}) \propto p(\mathbf{y} | \mathbf{X}, \beta) \cdot p(\beta)$$

$$\propto \left[\prod_{i=1}^n \frac{e^{y_i \beta^T \mathbf{x}_i}}{1 + e^{\beta^T \mathbf{x}_i}} \right] \cdot e^{-\frac{1}{2\sigma_0^2} \beta^T \beta}$$

393 The first term is the likelihood contribution
 394 as computed above, representing the fit of the
 395 model to the observed data, while the second
 396 term is the prior contribution, which penalizes
 397 coefficients with large magnitudes. The product
 398 of these two components balances data fit with
 399 regularization.

400 Once again, computational methods are
 401 needed due to the fact that the posterior distri-
 402 bution does not have a closed-form expression.

Parameter Tuning

Algorithm Overview

426 Since the posterior distribution $p(\beta | \mathbf{y}, \mathbf{X})$ lacks
 427 a closed-form expression, it cannot be sampled
 428 from directly using standard Gibbs sampling
 429 methods. Instead, the Metropolis algorithm is
 430 employed. This is a Markov Chain Monte Carlo
 431 (MCMC) technique that generates a sequence
 432 of samples $\beta^{(1)}, \beta^{(2)}, \dots, \beta^{(S)}$ that approximate
 433 draws from the posterior distribution. The key
 434 idea is to construct a Markov chain whose sta-
 435 tionary distribution is the target posterior. After
 436 the chain converges, samples can be used to es-
 437 timate posterior means, credible intervals, and
 438 other quantities of interest.

440 The Metropolis algorithm is a special case of
 441 the more general Metropolis-Hastings algorithm
 442 where the proposal distribution is symmetric—
 443 meaning the probability of proposing a move
 444 from state A to state B is the same as propos-
 445 ing a move from B to A. This symmetry sim-
 446 plifies the acceptance ratio calculation, as seen
 447 below, making the Metropolis algorithm partic-

448 ularly convenient when symmetric proposals are
 449 natural for the problem at hand.

450 **Proposal Distribution**

451 At each iteration k , the algorithm proposes a
 452 candidate value β^* from a symmetric proposal
 453 distribution centered at the current state $\beta^{(k)}$:

$$\beta^* | \beta^{(k)} \sim N(\beta^{(k)}, \Sigma_{\text{prop}})$$

454 This multivariate normal proposal is sym-
 455 metric because the probability of proposing
 456 $\beta^{(k)}$ given β^* is the same as the probabili-
 457 ty of proposing β^* given $\beta^{(k)}$. This sym-
 458 metry causes the proposal ratio to cancel in
 459 the Metropolis-Hastings acceptance probability,
 460 simplifying computations.

461 The choice of the proposal covariance matrix
 462 Σ_{prop} is critical for the algorithm's efficiency.

$$\Sigma_{\text{prop}} = \sigma_{\text{prop}}^2 (\mathbf{X}^T \mathbf{X})^{-1}$$

463 This form incorporates the correlation struc-
 464 ture among the features through the $\mathbf{X}^T \mathbf{X}^{-1}$
 465 term. When features are highly correlated, this
 466 proposal allows the algorithm to propose coor-
 467 dinated changes to multiple coefficients simulta-
 468 neously, improving exploration of the posterior
 469 distribution. The scalar tuning parameter σ_{prop}^2
 470 controls the overall scale of the proposals: larger
 471 values lead to bolder moves through the param-
 472 eter space, while smaller values result in more
 473 conservative steps.

474 The purpose of tuning the proposal variance
 475 is to balance two competing goals. If σ_{prop}^2 is too
 476 small, the algorithm takes tiny steps and accepts
 477 nearly every proposal, but explores the posterior
 478 very slowly, leading to a high acceptance rate
 479 but poor mixing. Conversely, if it is too large,
 480 the algorithm proposes extreme values that are
 481 frequently rejected again leading to slow explo-
 482 ration but with lower acceptance rate and poor
 483 mixing. Empirical research suggests that an ac-
 484 ceptance rate between 20% and 50% typically
 485 yields efficient exploration for multivariate prob-
 486 lems. σ_{prop}^2 is tuned to achieve rates within or
 487 close to this range.

488 **Acceptance Ratio**

489 At iteration k , after proposing β^* , it is decided
 490 whether to accept or reject it using the Metropo-
 491 lis acceptance ratio:

$$r = \frac{p(\mathbf{y} | \mathbf{X}, \beta^*) p(\beta^*)}{p(\mathbf{y} | \mathbf{X}, \beta^{(k)}) p(\beta^{(k)})}$$

492 This ratio compares the unnormalized posterior
 493 density at the proposed value β^* to the density
 494 at the current value $\beta^{(k)}$. Notice that the nor-
 495 malizing constant $p(\mathbf{y} | \mathbf{X})$ (which is intractable
 496 to compute) cancels in this ratio, allowing the
 497 evaluation of r using only the likelihood and
 498 prior, both of which are computable. If $r \geq 1$,
 499 the proposed value has higher posterior density
 500 and is always accepted. If $r < 1$, the proposed
 501 value is accepted with probability r , ensuring the
 502 chain can move to lower-density regions occasion-
 503 ally, which is necessary for convergence to the
 504 stationary distribution.

505 For numerical stability, the acceptance ratio
 506 is computed on the logarithmic scale. Probabili-
 507 ties in the likelihood can become extremely small
 508 (underflow) or large (overflow), but working with
 509 log probabilities avoids these issues. The log ac-
 510 ceptance ratio is:

$$\log r = \sum_{i=1}^n \left[y_i (\beta^{*T} \mathbf{x}_i - \beta^{(k)T} \mathbf{x}_i) - \log \frac{1 + \exp(\beta^{*T} \mathbf{x}_i)}{1 + \exp(\beta^{(k)T} \mathbf{x}_i)} \right] - \frac{1}{2\sigma_0^2} (\|\beta^*\|^2 - \|\beta^{(k)}\|^2)$$

511 The first term is the log-likelihood ratio,
 512 capturing how much better (or worse) the pro-
 513 posed parameters explain the observed data.
 514 The second term is the log-prior ratio, reflect-
 515 ing the change in prior plausibility. The decision
 516 rule is:

$$\beta^{(k+1)} = \begin{cases} \beta^* & \text{if } \log u \leq \log r \\ \beta^{(k)} & \text{else} \end{cases}$$

517 where $u \sim \text{Uniform}(0, 1)$. This acceptance mech-
 518 anism ensures detailed balance, guaranteeing
 519 that the Markov chain converges to the target
 520 posterior distribution.

521 **Tuning the Proposal Variance**

522 Before running the full MCMC chain on the
 523 model, it is essential to select an appropriate
 524 value for σ_{prop}^2 . This tuning process involves run-
 525 ning short pilot chains, with different candidate
 526 values, and monitoring the acceptance rate. The
 527 goal is to find a value that produces an accep-
 528 tance rate between 20% and 50%, which has
 529 been shown empirically to provide efficient ex-
 530 ploration of the posterior in multivariate set-
 531 tings.

532 Thus, a grid of candidate values is tested
 533 by running short MCMC chains for each value
 534 and recording the acceptance rate. The opti-
 535 mal choice is the value whose acceptance rate
 536 is closest to 35%, which is the midpoint of the
 537 desired range, since there can be times where
 538 the rates may not be perfectly within the range.
 539 This tuning step is computationally inexpensive
 540 relative to the full analysis and substantially im-
 541 proves the quality of posterior samples by ensur-
 542 ing the chain mixes well and explores the poste-
 543 rior efficiently.

544 Once the optimal σ_{prop}^2 is identified, the full
 545 MCMC sampler is run for a larger number of
 546 iterations using this tuned value. The result-
 547 ing samples, after discarding an initial burn-in
 548 period where the chain adjusts from the prior
 549 value, constitute approximate draws from the
 550 posterior distribution and form the basis for all
 551 subsequent inference.

552 The values being tested as candidates for
 553 σ_{prop}^2 are $\{0.5, 1, 2, 5, 10, 25, 50, 100\}$. After run-
 554 ning chains for 2,000 iterations, the following ac-
 555 ceptance rates are computed.

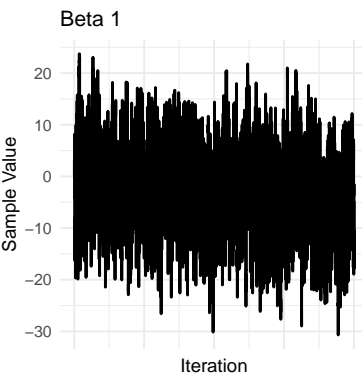
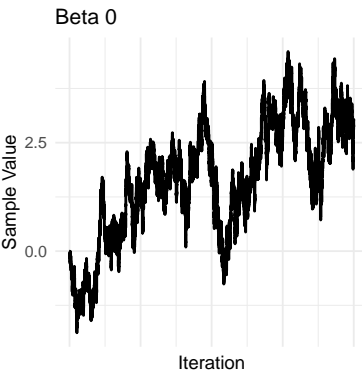
```
556 ## sigma2_prop acceptance_rate
557 ## 1          0.5      0.645
558 ## 2          1.0      0.579
559 ## 3          2.0      0.482
560 ## 4          5.0      0.315
561 ## 5         10.0     0.176
562 ## 6         25.0     0.066
563 ## 7         50.0     0.028
564 ## 8        100.0    0.025
```

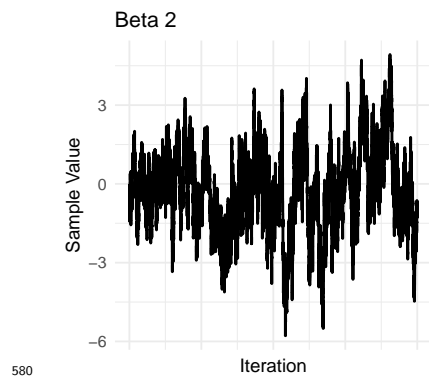
565 The value with acceptance rate closest to 579

566 35% is 5, which will be chosen as the optimal
 567 value.

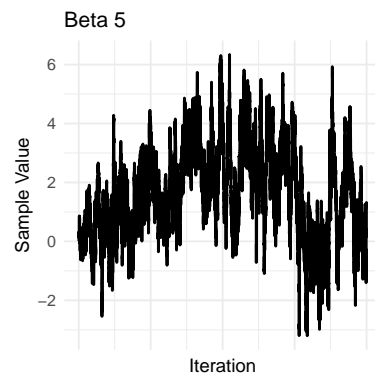
568 **Constructing the Full Model 569 using MCMC Diagnostics**

570 Now that the parameter has been tuned to the
 571 most optimal value, the number of iterations can
 572 be increased to 20,000 with the parameter set to
 573 $\sigma_{\text{prop}}^2 = 5.0$. The diagnostic traceplots and au-
 574 tocorrelation function plots can be plotted after
 575 this to evaluate the coefficients, and determine
 576 the amount of burn-in and thinning needed to
 577 create the best version of the full model.

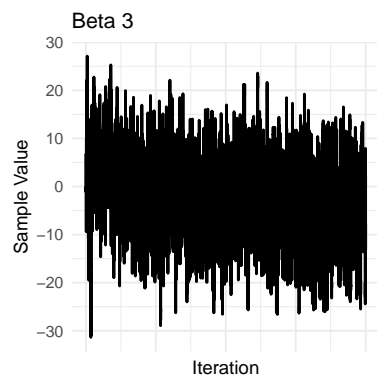




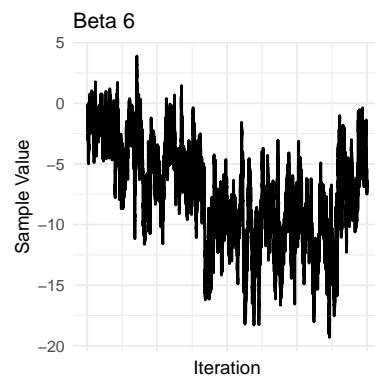
580



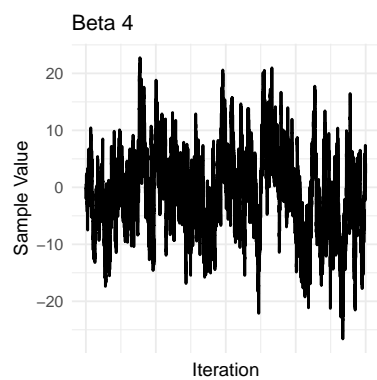
583



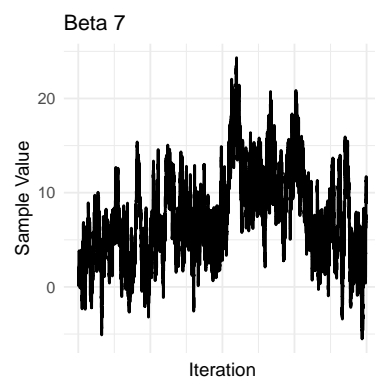
581



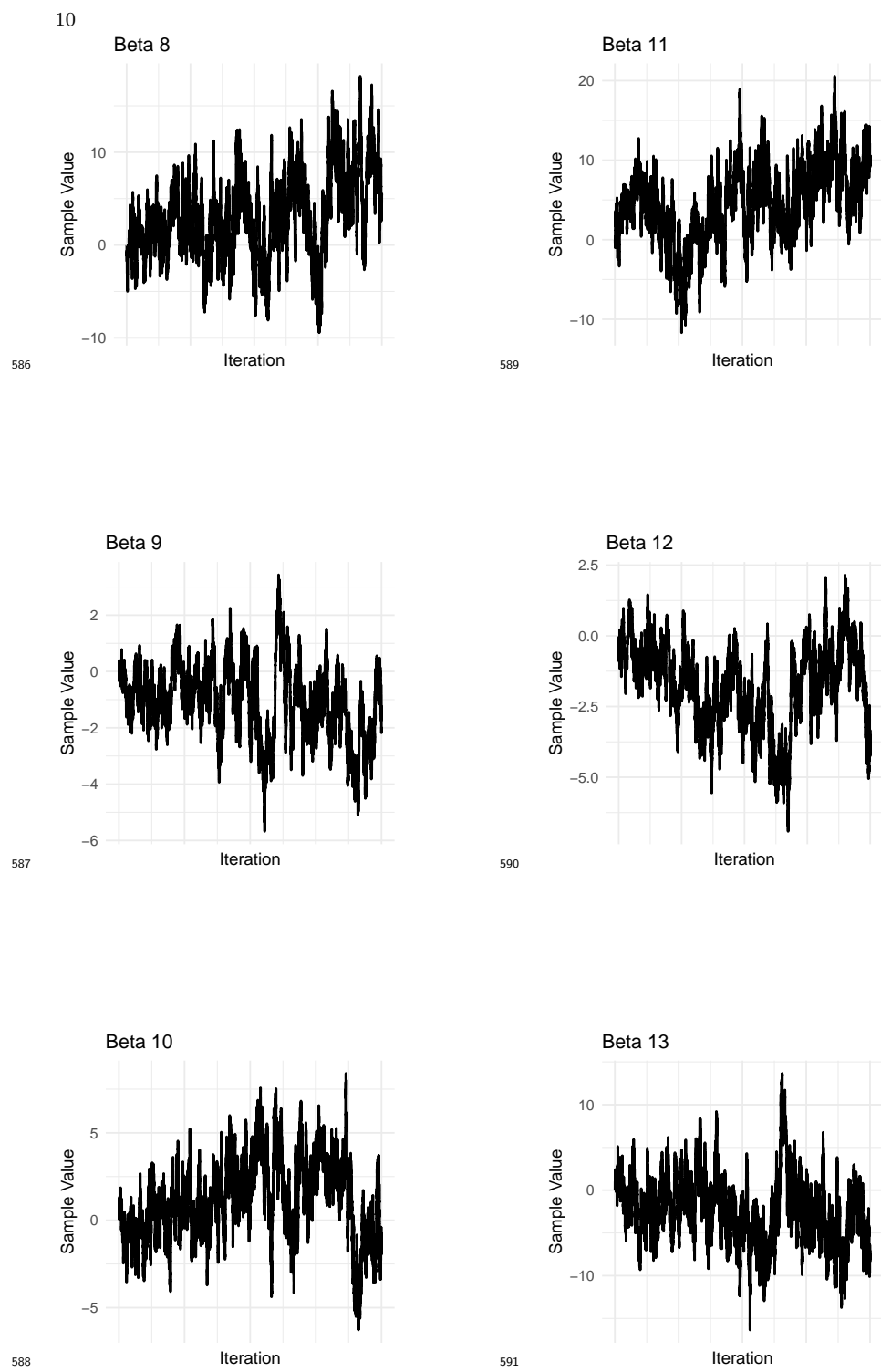
584

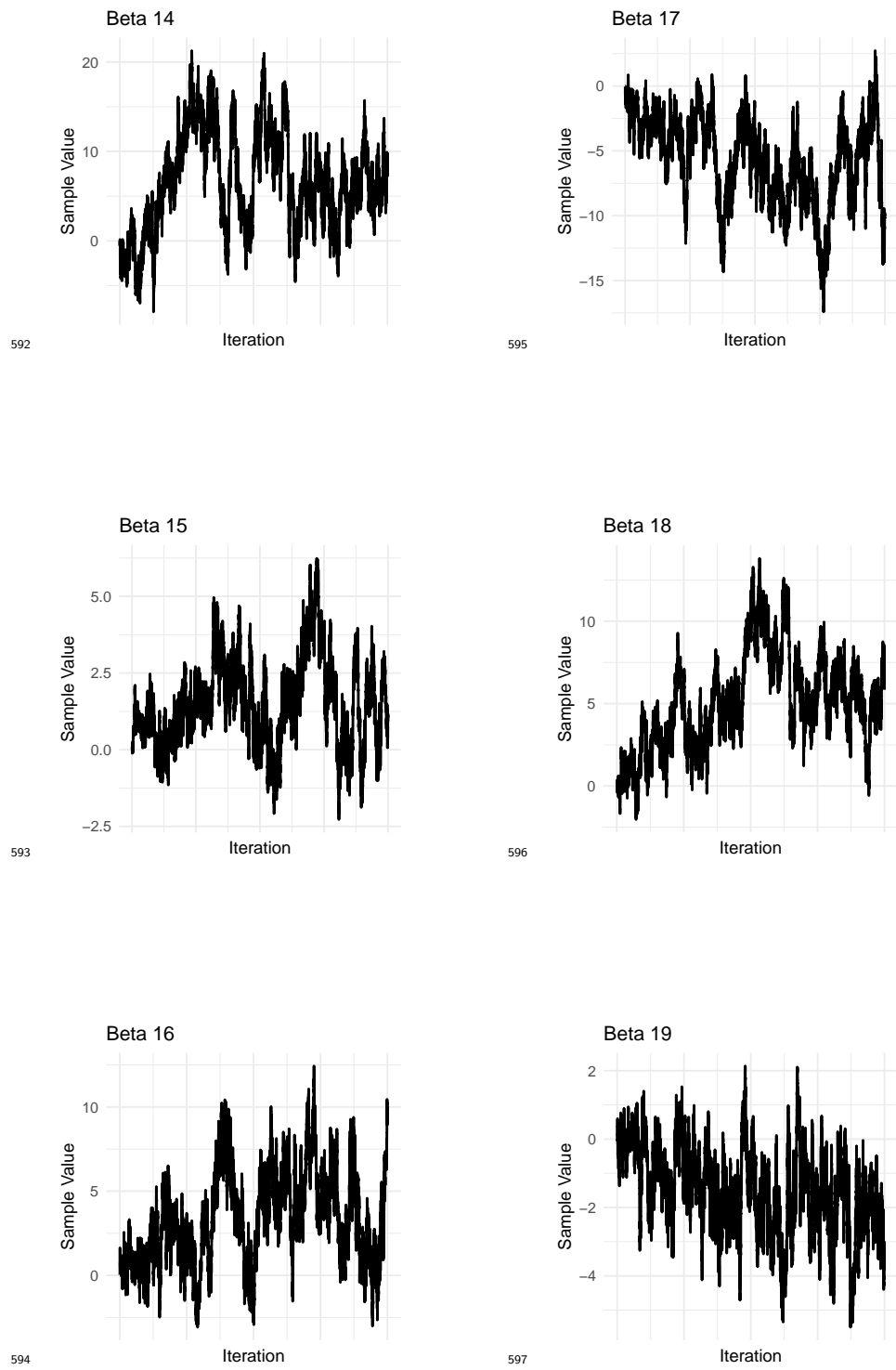


582

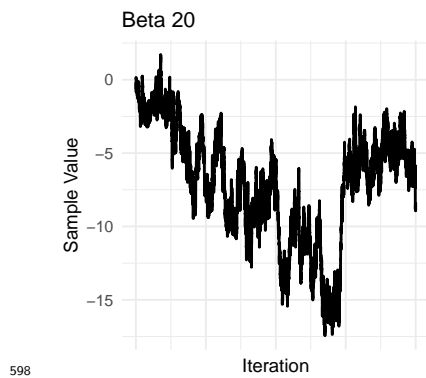


585

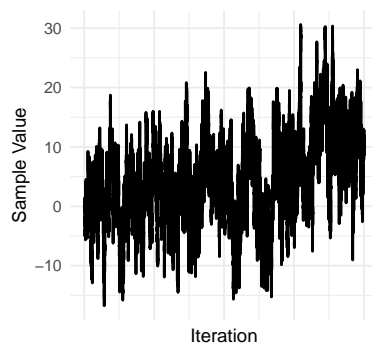




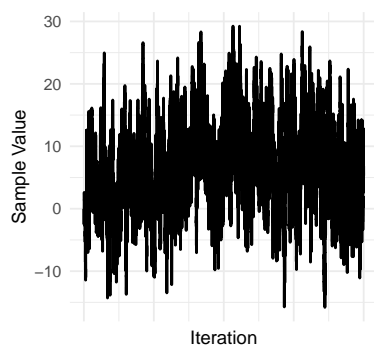
12



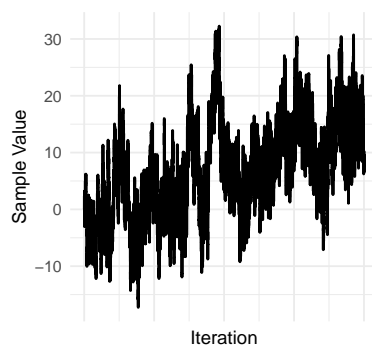
Beta 23



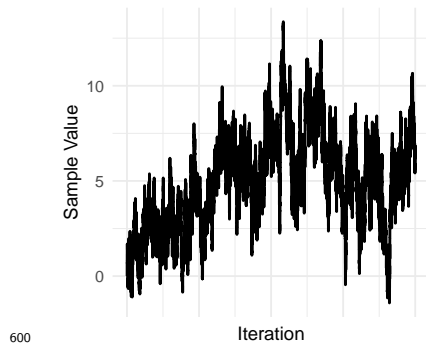
Beta 21



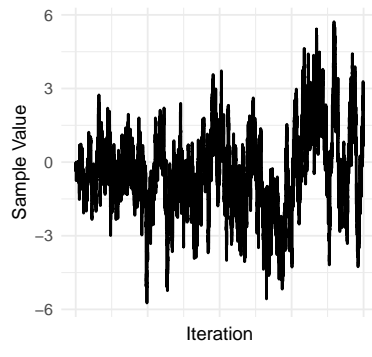
Beta 24

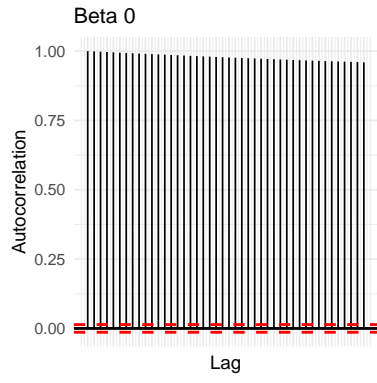
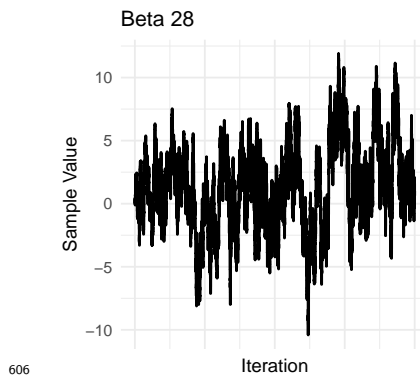
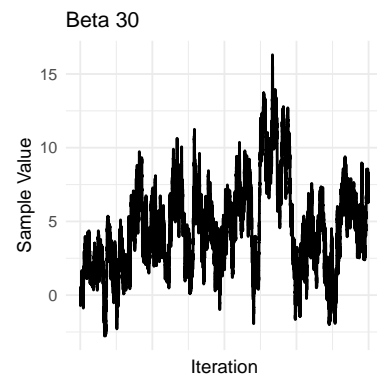
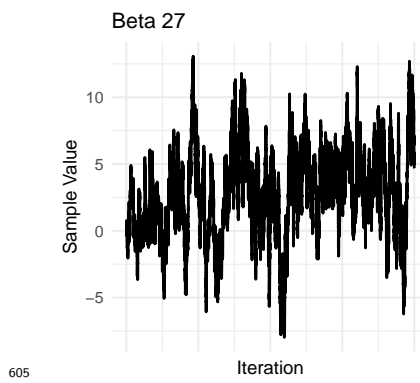
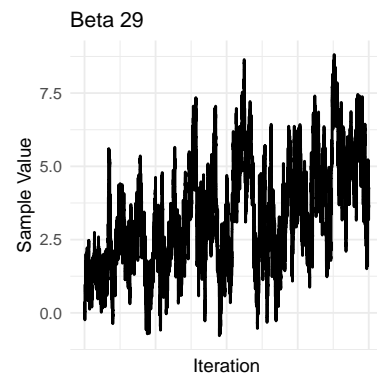
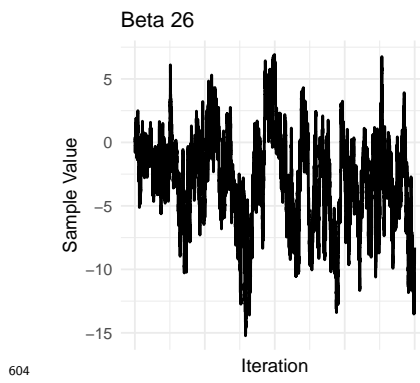


Beta 22

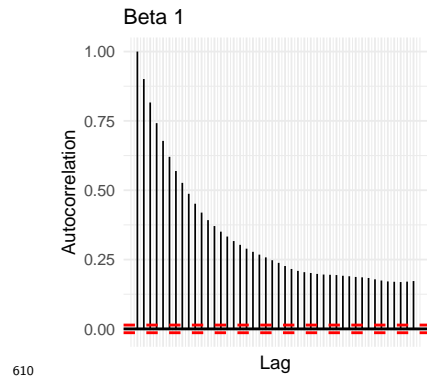


Beta 25

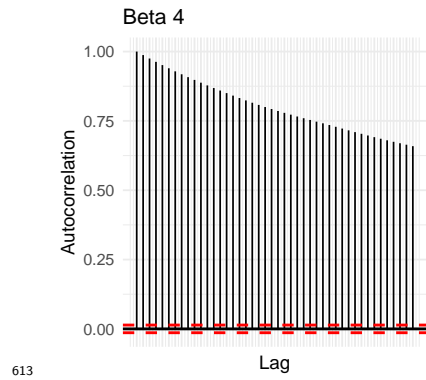




14

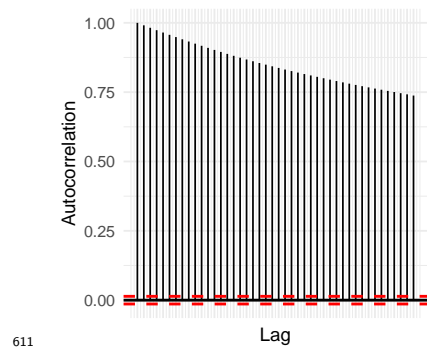


610



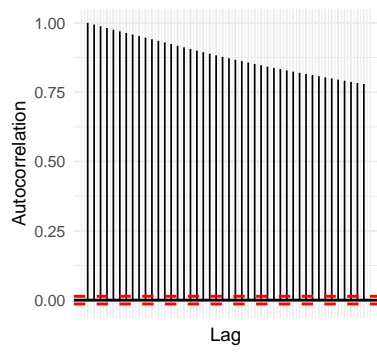
613

Beta 2



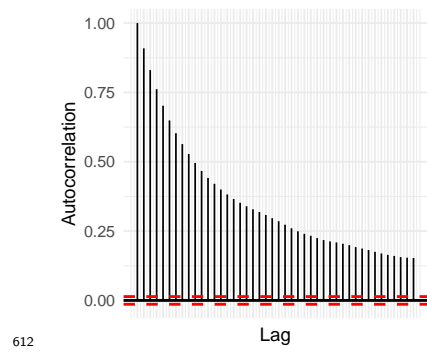
611

Beta 5



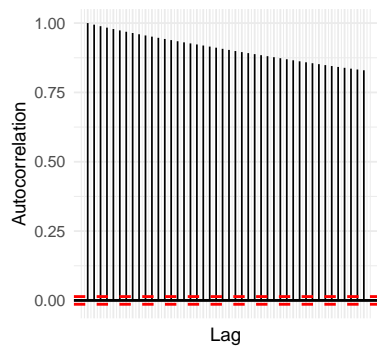
614

Beta 3

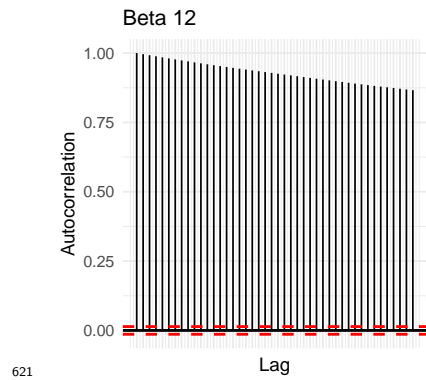
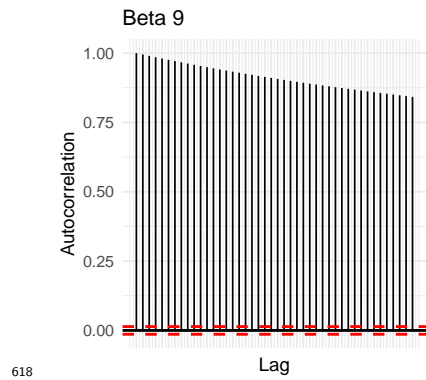
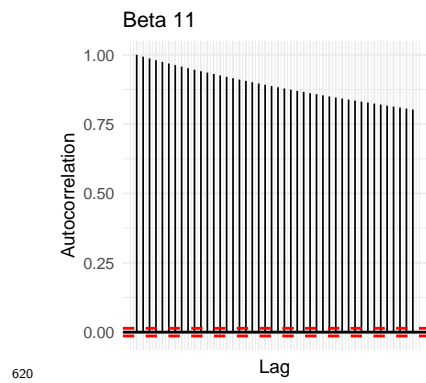
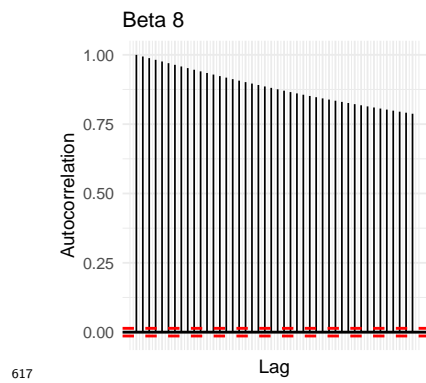
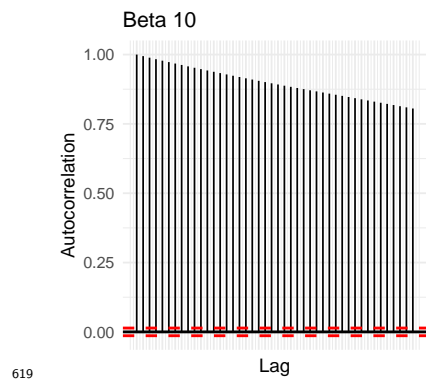
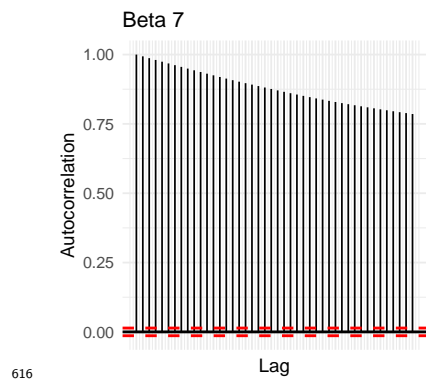


612

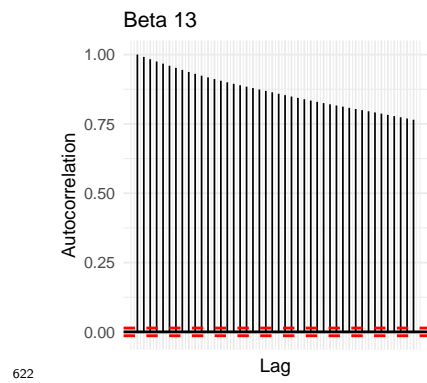
Beta 6



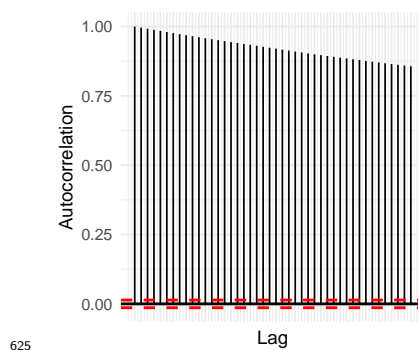
615



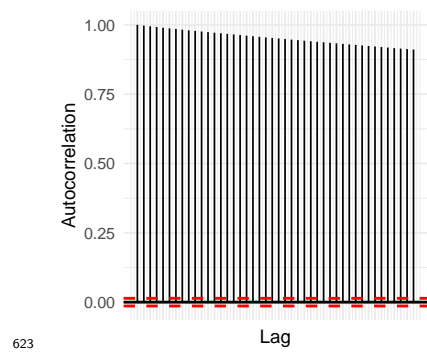
16



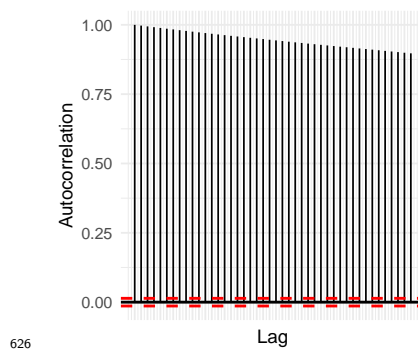
Beta 16



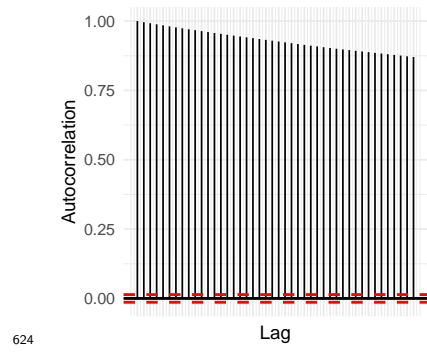
Beta 14



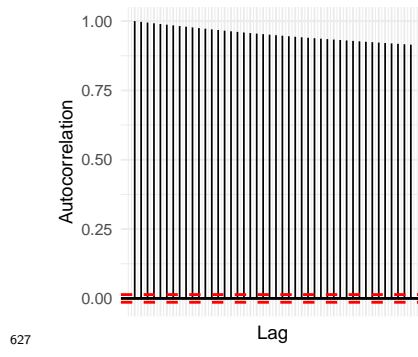
Beta 17

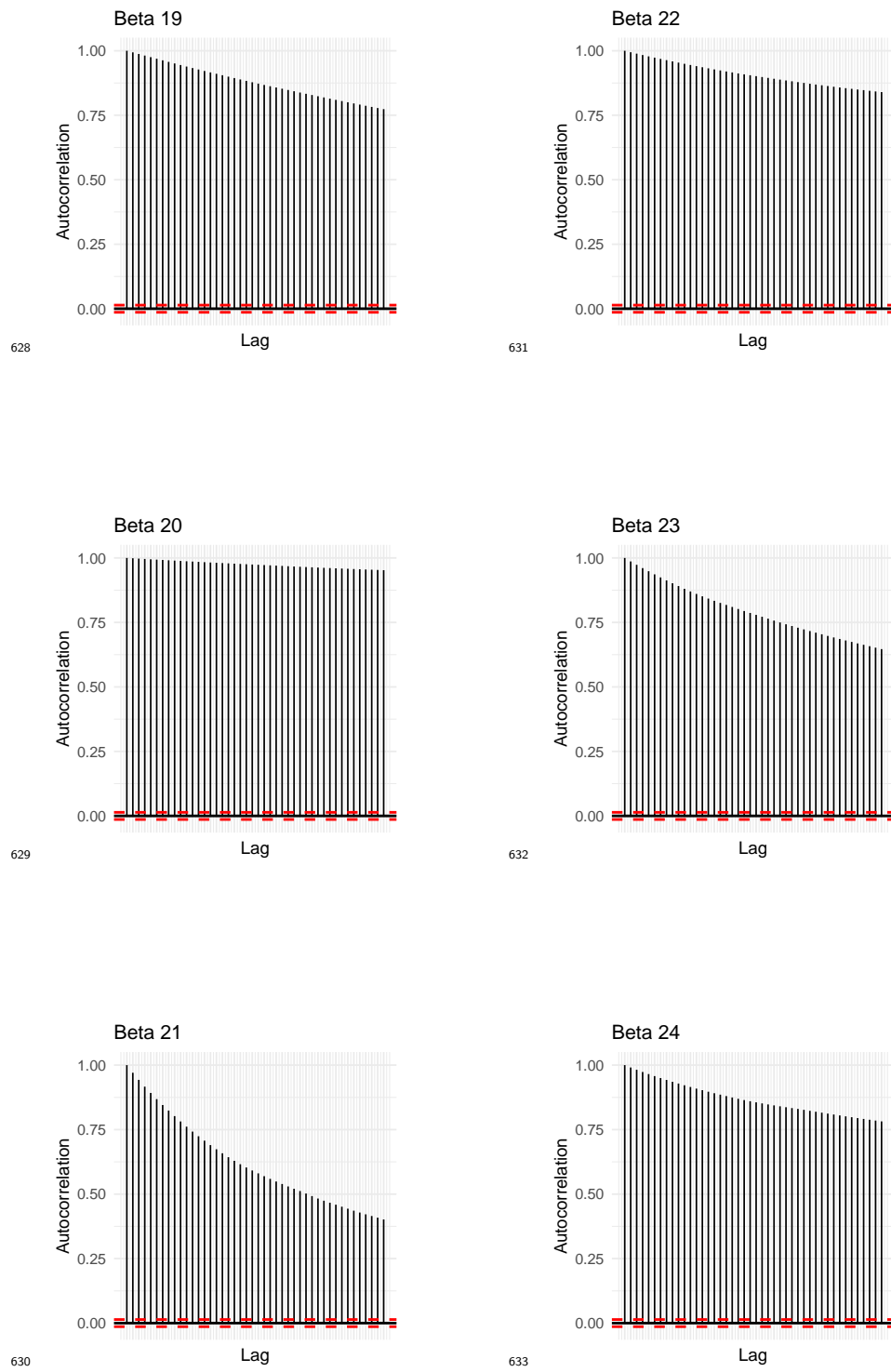


Beta 15

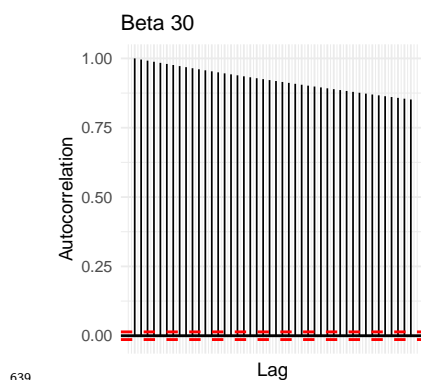
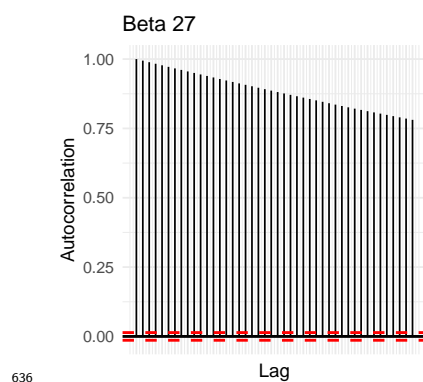
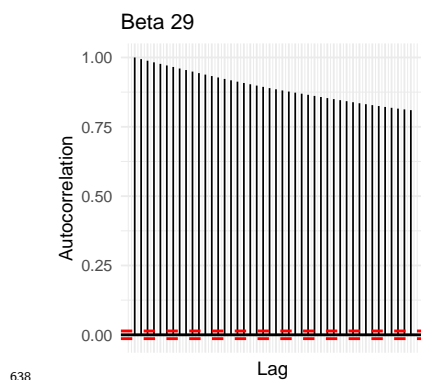
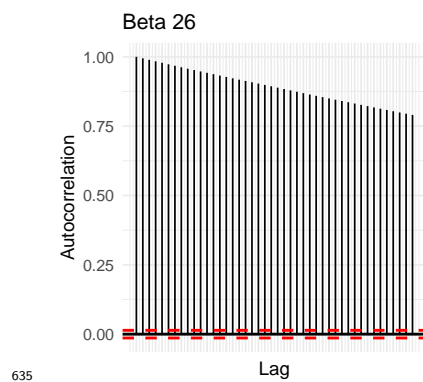
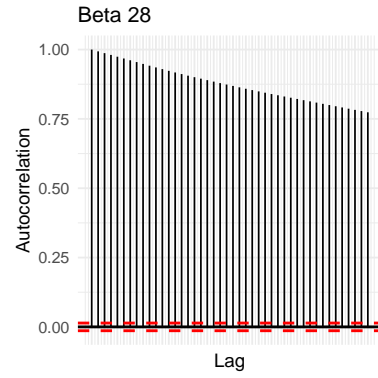
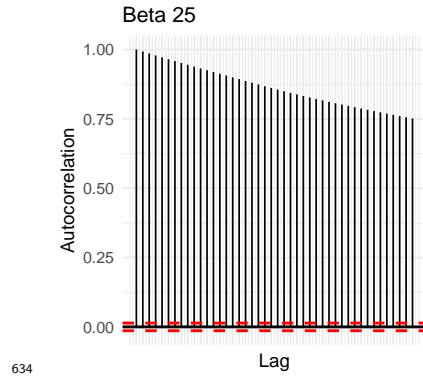


Beta 18





18



640 Before interpreting the plots, one needs to
 641 adjust the β samples by burning-in and thinning
 642 them. Upon taking a look at the traceplots,
 643 it looks like the chains take about the first 1,000
 644 iterations to start converging, so the first thou-
 645 sand samples are discarded. Thinning may not
 646 be a good idea, since it will not make a differ-
 647 ence, considering there is extremely high auto-

648 correlation for the samples of all β_i . Upon test- 696 ## 3 -3.4856376 2.9946985
 649 ing, the values of the coefficients do not change 697 ## 4 -18.1270565 12.4704710
 650 by a lot either. As for the diagnostics of this 698 ## 5 -15.0994008 14.3428624
 651 MCMC simulation, good mixing is only seen in 699 ## 6 -1.4481216 4.7211568
 652 a few coefficients, and not all. 700 ## 7 -15.4038902 -0.6953401
 653 The posterior means, 95% credible intervals, 701 ## 8 -0.5706768 17.7769508
 654 and significance of the various features are in 702 ## 9 -4.9496555 12.3973170
 655 the table below. Significance is determined by 703 ## 10 -3.8871346 1.3998645
 656 whether zero is included within the significance 704 ## 11 -3.3940364 5.6095899
 657 interval. If zero is not included, this means that 705 ## 12 -5.3871781 13.5534819
 658 there is a clear direction of the effect of the given 706 ## 13 -5.0118690 0.6785438
 659 variable on the malignancy of the mass, and the 707 ## 14 -9.8685213 6.5431827
 660 variable is likely to be significant. 708 ## 15 -3.3532157 17.2591935
 709 ## 16 -0.9753628 4.5373823
 661 ## Feature Posterior.Mean 710 ## 17 -1.4584953 9.1899987
 662 ## 1 radius1 1.7754860 711 ## 18 -13.2243149 -0.4488643
 663 ## 2 texture1 -3.4493988 712 ## 19 0.4025852 11.2145611
 664 ## 3 perimeter1 -0.2689530 713 ## 20 -4.2082020 0.7855442
 665 ## 4 area1 -2.6283274 714 ## 21 -15.6389864 -1.2344497
 666 ## 5 smoothness1 -0.7781131 715 ## 22 -6.9512896 20.8152030
 667 ## 6 compactness1 1.6904161 716 ## 23 0.7802777 10.1108130
 668 ## 7 concavity1 -7.6811684 717 ## 24 -9.7288741 19.2618953
 669 ## 8 concave_points1 7.6316236 718 ## 25 -7.6918795 23.9887362
 670 ## 9 symmetry1 3.2774668 719 ## 26 -3.7978384 3.3578309
 671 ## 10 fractal_dimension1 -1.0895585 720 ## 27 -10.7738418 4.0033313
 672 ## 11 radius2 1.2469487 721 ## 28 -4.0465014 9.5626004
 673 ## 12 texture2 -1.8238974 722 ## 29 -5.1513972 7.9451506
 674 ## 13 perimeter2 -2.5221828 723 ## 30 0.3100122 6.9465286
 675 ## 14 area2 6.9847849 724 ## 31 -0.4953099 11.7846683
 676 ## 15 smoothness2 1.5147851
 677 ## 16 compactness2 3.4526549
 678 ## 17 concavity2 -5.8965451
 679 ## 18 concave_points2 5.2522748
 680 ## 19 symmetry2 -1.5805192
 681 ## 20 fractal_dimension2 -7.3571682
 682 ## 21 radius3 6.6663185
 683 ## 22 texture3 5.1753524
 684 ## 23 perimeter3 4.5529981
 685 ## 24 area3 7.3644317
 686 ## 25 smoothness3 -0.4141473
 687 ## 26 compactness3 -3.0742975
 688 ## 27 concavity3 2.9748868
 689 ## 28 concave_points3 1.3182111
 690 ## 29 symmetry3 3.3746718
 691 ## 30 fractal_dimension3 4.7492725
 692 ## 31 Lower.CI Upper.CI Significance
 693 ## 1 -0.8609714 3.8724485 No
 694 ## 2 -18.2375516 11.6857163 No

725 Model selection within the Bayesian frame-
 726 work is still required, however. Variables selected
 727 by “significance” as done in linear regression, do
 728 not show good mixing in the traceplots.

729 **Variable Selection**

730 In the previous section, all 30 regression coeffi-
 731 cients were estimated simultaneously. However,
 732 not all features may be equally important for
 733 predicting malignancy. Including irrelevant fea-
 734 tures can lead to overfitting and reduced inter-
 735 pretability. Bayesian variable selection provides
 736 a principled framework for identifying which fea-
 737 tures are most informative while accounting for
 738 uncertainty in the selection process itself.

739 **Model Formulation**

740 Rather than estimating a single model, all possi-
 741 ble subsets of features are considered. The data
 742 determines which features should be included.
 743 Binary indicator variables $\mathbf{z} = (z_1, \dots, z_p)$ are
 744 introduced where $z_j \in \{0, 1\}$ indicates whether
 745 feature j is included in the model:

$$\text{logit}(\theta_i) = b_0 + \sum_{j=1}^{30} z_j b_j x_{i,j}$$

746 If $z_j = 1$, feature j is included in the model,
 747 contributing $b_j x_{i,j}$ to the linear predictor. If
 748 $z_j = 0$, feature j is excluded from the model,
 749 contributing nothing (effectively $\beta_j = 0$).

750 The intercept b_0 is always included (no in-
 751 dicator variable). The joint parameter vector is
 752 now $\boldsymbol{\theta} = (\mathbf{z}, \mathbf{b})$, where $\mathbf{b} = (b_0, b_1, \dots, b_{30})$ are
 753 the regression coefficients. Importantly, \mathbf{b} rep-
 754 resents the coefficients if the corresponding fea-
 755 tures were included—the actual effect is $j\beta_j =$
 756 $z_j \cdot b_j$.

772 \mathbf{b} —they can be updated separately within each
 773 MCMC iteration using a two-step Metropolis-
 774 Hastings procedure.

775 First, \mathbf{z} is updated given current \mathbf{b} . At itera-
 776 tion k , a new indicator vector \mathbf{z}^* is proposed by
 777 randomly flipping each indicator with probabili-
 778 ty $p_{\text{flip}} = 0.2$:

$$z_j^* = \begin{cases} z_j^{(k)} & \text{with } p_{\text{flip}} = 0.8 \text{ (no flip)} \\ 1 - z_j^{(k)} & \text{with } p_{\text{flip}} = 0.2 \text{ (flip)} \end{cases}$$

779 This proposal is symmetric: the probability of
 780 proposing \mathbf{z}^* from $\mathbf{z}^{(k)}$ equals the probability
 781 of proposing $\mathbf{z}^{(k)}$ from \mathbf{z}^* . The acceptance ratio
 782 simplifies to:

$$r_z = \frac{p(\mathbf{y} | \mathbf{X}, \mathbf{z}^*, \mathbf{b}^{(k)})}{p(\mathbf{y} | \mathbf{X}, \mathbf{z}^{(k)}, \mathbf{b}^{(k)})}$$

783 Next, \mathbf{b} is updated given current \mathbf{z} . After
 784 updating \mathbf{z} , the coefficients \mathbf{z} are updated using
 785 the same symmetric normal proposal as in the
 786 full model:

$$\mathbf{b}^* \sim N(\mathbf{b}^{(k)}, \boldsymbol{\Sigma}_{\text{prop}})$$

787 where $\boldsymbol{\Sigma}_{\text{prop}} = 0.5 \cdot (\mathbf{X}^T \mathbf{X})^{-1}$. The acceptance
 788 ratio is:

$$r_b = \frac{p(\mathbf{y} | \mathbf{X}, \mathbf{z}^{(k+1)}, \mathbf{b}^*) p(\mathbf{b}^*)}{p(\mathbf{y} | \mathbf{X}, \mathbf{z}^{(k+1)}, \mathbf{b}^{(k)}) p(\mathbf{b}^{(k)})}$$

789 Note that this ratio is evaluated using the up-
 790 dated indicator vector $\mathbf{z}^{(k+1)}$ from the first step.
 791 This ensures that the coefficient updates are con-
 792 ditioned on the current model structure.

793 **Computing the Effective Coefficient Vector**

794 For likelihood evaluation, the effective coefficient
 795 vector is computed:

$$\boldsymbol{\beta}_{\text{effective}} = \begin{bmatrix} b_0 \\ z_1 b_1 \\ z_2 b_2 \\ \vdots \\ z_{30} b_{30} \end{bmatrix}$$

757 **Prior Specifications**

758 One must specify prior distributions for both the
 759 coefficients \mathbf{b} and the indicators \mathbf{z} . For the coeffi-
 760 cients, one must use the same weakly informative
 761 multivariate normal prior as before:

$$\mathbf{b} \sim \mathcal{N}(\mathbf{0}, \sigma_b^2 \mathbf{I}_{31}), \quad \sigma_b^2 = 100$$

762 For the indicators, equal prior probability is as-
 763 signed to inclusion or exclusion:

$$p(z_j = 1) = 0.5, \quad \text{independently for } j = 1, \dots, 30$$

764 This uniform prior on each z_j implies equal
 765 prior probability across all $2^{30} \approx 1.07$ billion
 766 possible models. No *a priori* assumption is made
 767 about which features are important, allowing the
 768 data to guide the selection.

769 **Metropolis-Hastings Algorithm**

770 Since there now are two types of parameters—
 771 discrete indicators \mathbf{z} and continuous coefficients

796 When $z_j = 0$, the corresponding coefficient is zeroed out, effectively excluding that feature from the model.

799 After running the MCMC sampler, samples $\mathbf{z}^{(1)}, \mathbf{z}^{(2)}, \dots, \mathbf{z}^{(S)}$ are obtained of the indicator variables. The posterior inclusion probability for feature j is simply the proportion of iterations where $z_j = 1$:

$$P(z_j = 1 | \mathbf{y}, \mathbf{X}) \approx \frac{1}{S - S_{\text{burnin}}} \sum_{s=S_{\text{burnin}}+1}^S z_j^{(s)}$$

804 This probability quantifies the posterior belief that feature j should be included in the model. Features with high inclusion probabilities (e.g., > 0.5) are strongly supported by the data, while features with low probabilities can be considered unimportant. All features and their inclusion probabilities are displayed below:

```

838 ## 10 fractal_dimension1
839 ## 22 texture3
840 ## 24 area3
841 ## 26 compactness3
842 ## Inclusion_Probability
843 ## 2 1.00000000
844 ## 5 1.00000000
845 ## 6 1.00000000
846 ## 17 1.00000000
847 ## 21 1.00000000
848 ## 27 1.00000000
849 ## 3 0.96957895
850 ## 4 0.86126316
851 ## 15 0.72673684
852 ## 20 0.70757895
853 ## 11 0.67263158
854 ## 29 0.61726316
855 ## 18 0.58226316
856 ## 28 0.54289474
857 ## 1 0.53542105
858 ## 14 0.52884211
859 ## 13 0.49836842
860 ## 7 0.48378947
861 ## 23 0.26952632
862 ## 9 0.24700000
863 ## 8 0.21700000
864 ## 16 0.19236842
865 ## 25 0.12589474
866 ## 19 0.11815789
867 ## 12 0.08057895
868 ## 30 0.06752632
869 ## 10 0.00000000
870 ## 22 0.00000000
871 ## 24 0.00000000
872 ## 26 0.00000000
873 The important features are as follows:
874 ## [1] "texture1"
875 ## [2] "smoothness1"
876 ## [3] "compactness1"
877 ## [4] "concavity2"
878 ## [5] "radius3"
879 ## [6] "concavity3"
880 ## [7] "radius2"
881 ## [8] "concave_points3"
882 ## [9] "radius1"
883 ## [10] "perimeter2"
884 ## [11] "concavity1"
```

```

885 ## [12] "symmetry1"                               928 ## 28      concavity3    1.00000000
886 ## [13] "concave_points1"                      929 ## 29      concave_points3 0.54289474
887 ## [14] "fractal_dimension1"                   930 ## 30      symmetry3     0.61726316
888 ## [15] "texture3"                            931 ## 31 fractal_dimension3 0.06752632
889 ## [16] "area3"                                932 ## Post_Mean   CI_Lower
890 Posterior Estimates for the Selected Model          933 ## 1 -0.36995562 -1.6628080
891 To obtain coefficient estimates that account for 934 ## 2 -1.65944780 -14.4222991
892 variable selection uncertainty, the effective coef- 935 ## 3 2.67392396 1.5502169
893 ficients for each MCMC sample are computed by 936 ## 4 -1.58125765 -13.6273034
894 multiplying the coefficient values by their corre- 937 ## 5 -0.75663039 -10.5585875
895 sponding indicators: 938 ## 6 1.88475774 0.1327450
939 ## 7 -3.40528590 -6.6355650
940 ## 8 1.50767820 -0.0317417
941 ## 9 0.12862344 -3.0097286
942 ## 10 -0.29223032 -1.9698534
943 ## 11 0.00000000 0.0000000
944 ## 12 1.93842218 -1.8443072
945 ## 13 -0.02025018 -0.4594021
946 ## 14 -0.40212524 -4.8276812
947 ## 15 2.49403402 0.0000000
948 ## 16 0.94360290 0.0000000
949 ## 17 -0.03647296 -1.2877484
950 ## 18 -3.46134538 -6.2190711
951 ## 19 1.65461316 -0.0889657
952 ## 20 0.11877276 0.0000000
953 ## 21 -1.49637658 -3.4927494
954 ## 22 12.17590190 1.1319955
955 ## 23 0.00000000 0.0000000
956 ## 24 0.13992429 -7.4664087
957 ## 25 0.00000000 0.0000000
958 ## 26 -0.08956376 -1.4202561
959 ## 27 0.00000000 0.0000000
960 ## 28 5.44035795 1.0965329
961 ## 29 2.35460982 0.0000000
962 ## 30 0.80671130 0.0000000
963 ## 31 0.03674546 0.0000000
964 ## CI_Upper
965 ## 1 0.8728454937
966 ## 2 8.0885531493
967 ## 3 3.8189359532
968 ## 4 12.9706383321
969 ## 5 10.4023848826
970 ## 6 3.4902249693
971 ## 7 0.0566711468
972 ## 8 6.4329458271
973 ## 9 3.8544998518
974 ## 10 0.0000000000
975 ## 11 0.0000000000
976 ## 12 7.4869133881
977 ## 13 0.0000000000

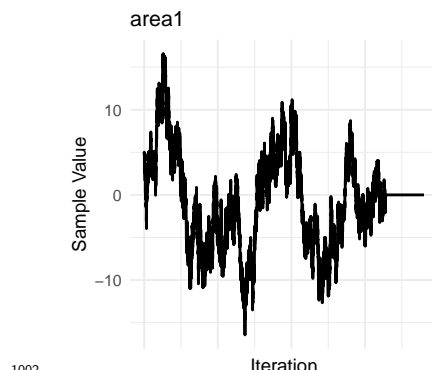
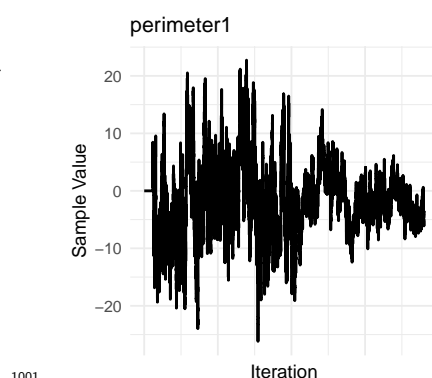
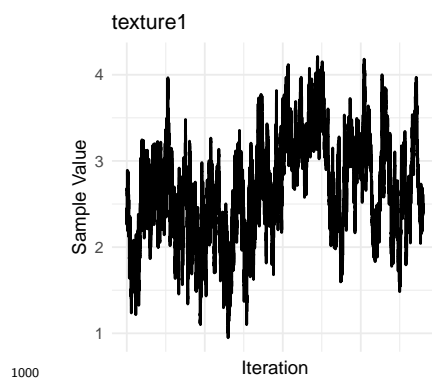
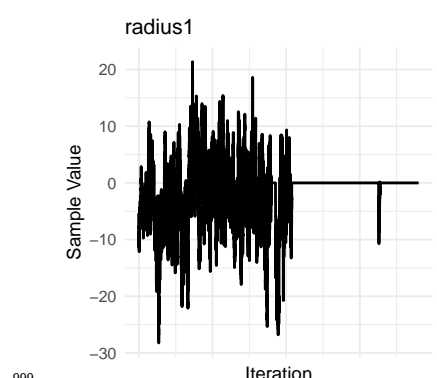
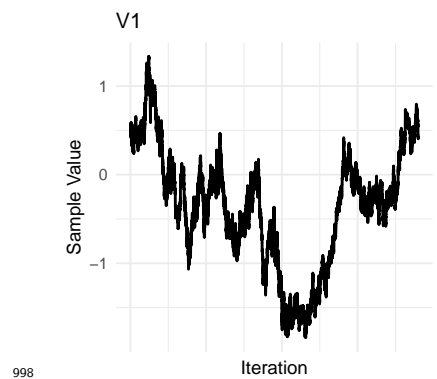
```

```

978 ## 14 3.4268658484
979 ## 15 7.1156958488
980 ## 16 2.3140542685
981 ## 17 0.8125925790
982 ## 18 -1.6477107371
983 ## 19 5.2973520748
984 ## 20 1.2408535966
985 ## 21 0.3110486179
986 ## 22 20.2764899183
987 ## 23 0.0000000000
988 ## 24 8.7106883638
989 ## 25 0.0000000000
990 ## 26 0.0001140985
991 ## 27 0.0000000000
992 ## 28 8.7035620731
993 ## 29 7.6234487248
994 ## 30 2.5257268242
995 ## 31 0.8500493773

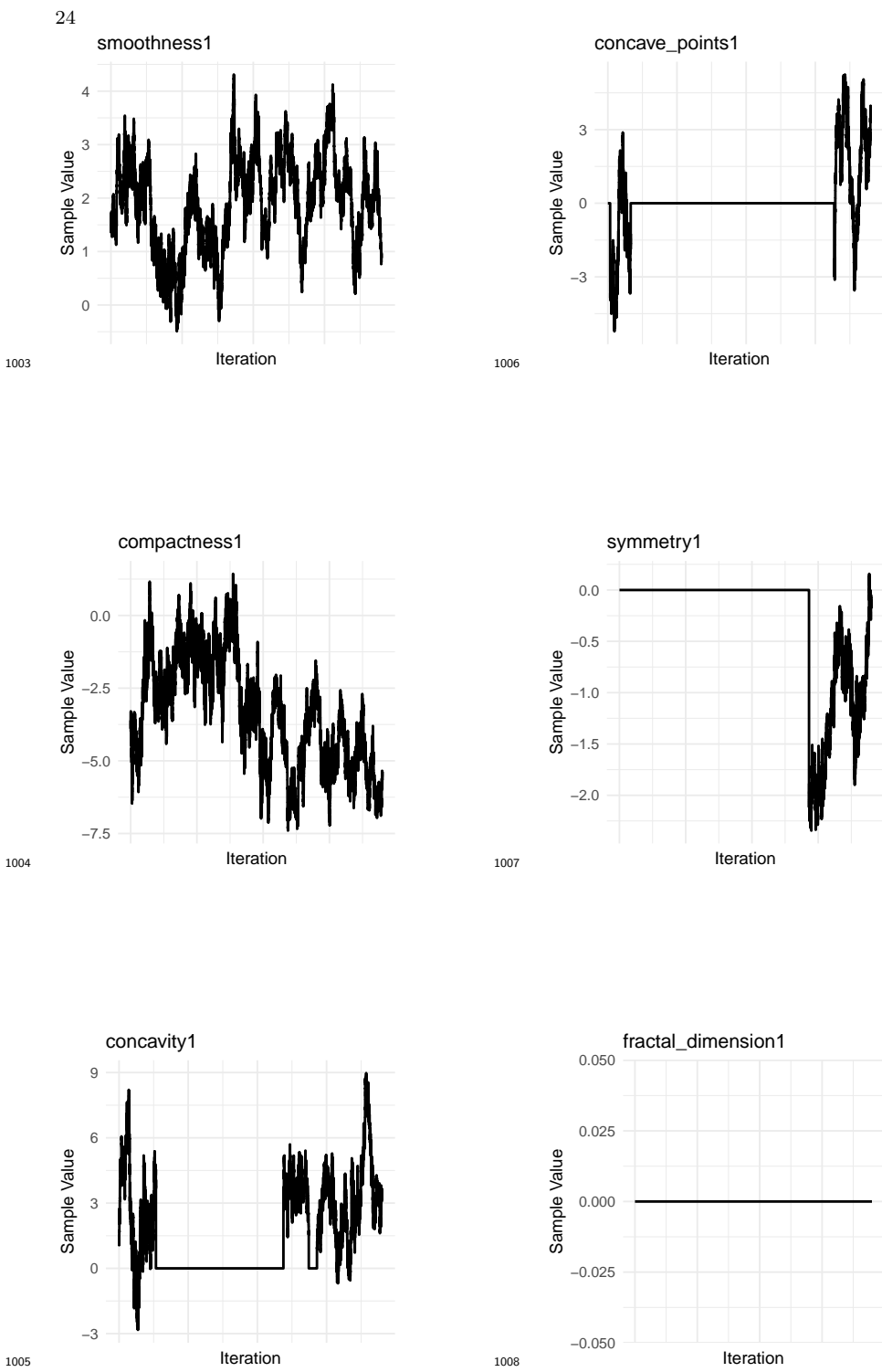
```

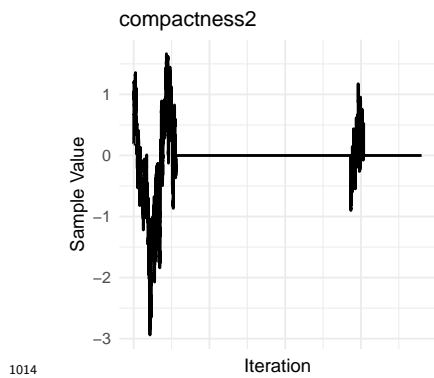
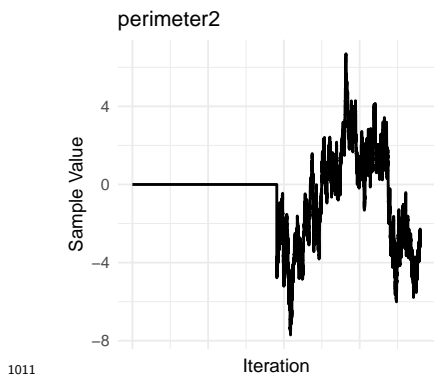
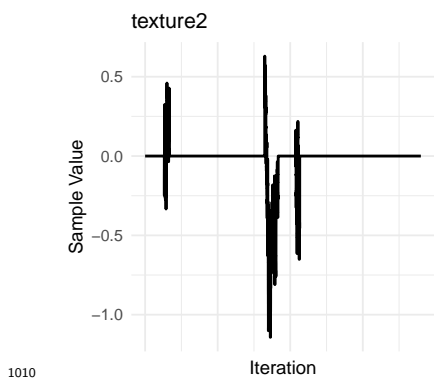
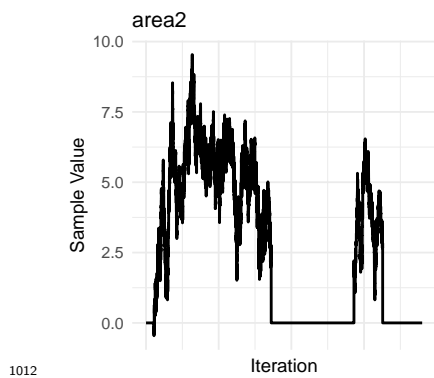
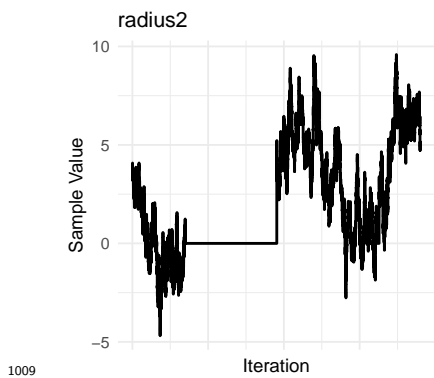
996 The traceplots for the coefficients are as fol-
997 lows:

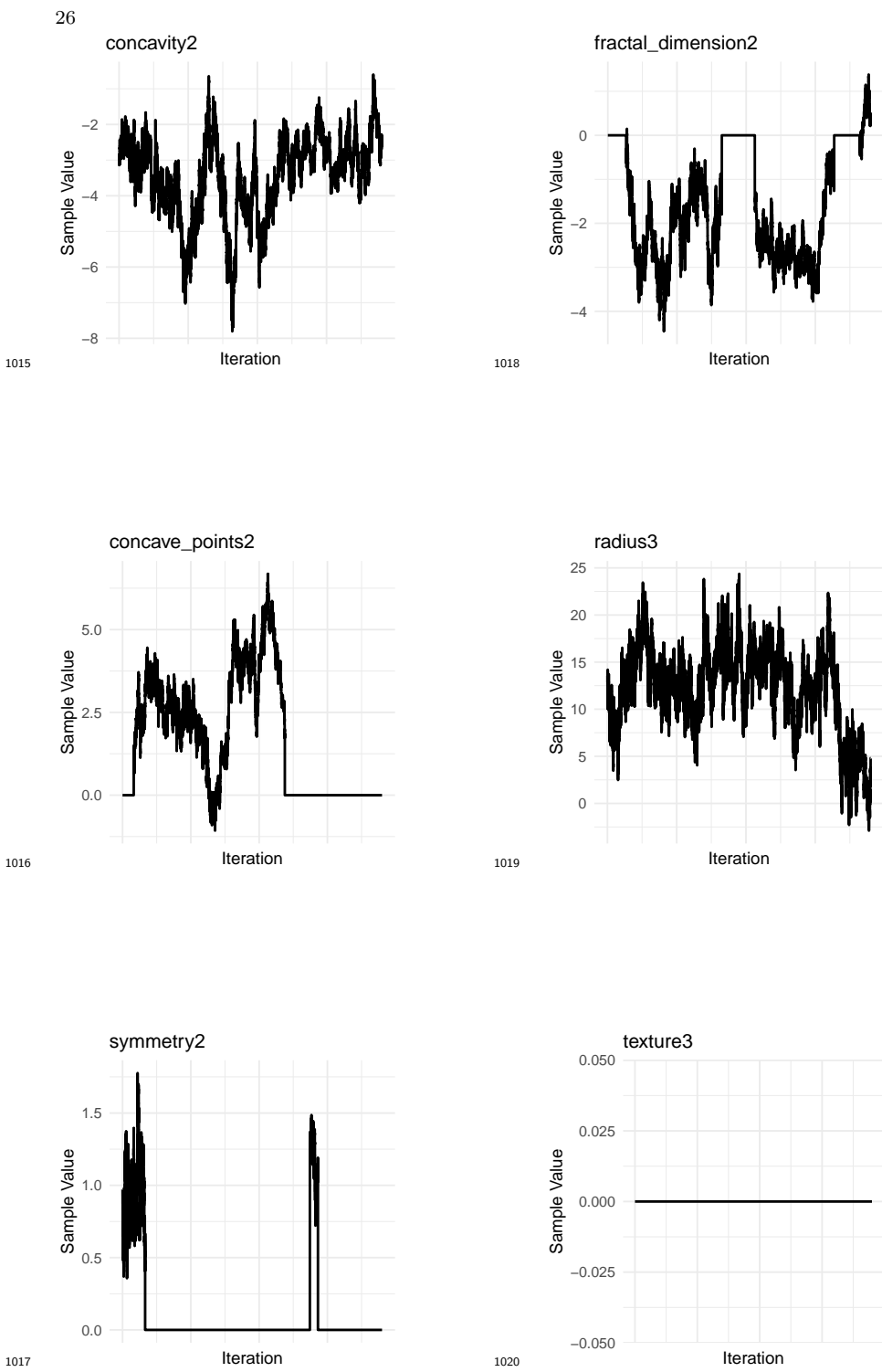


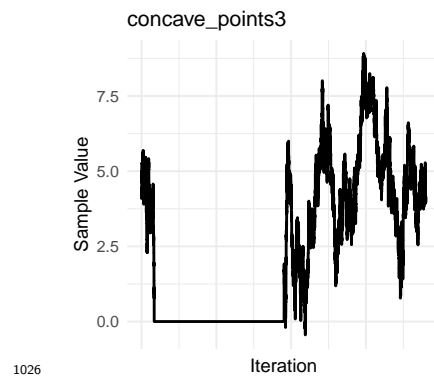
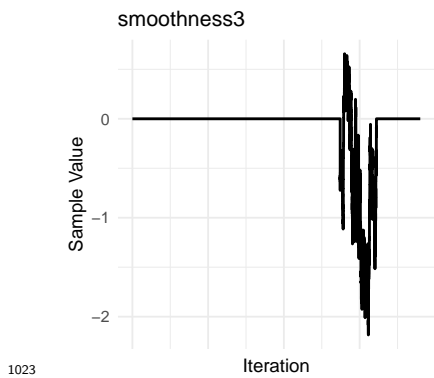
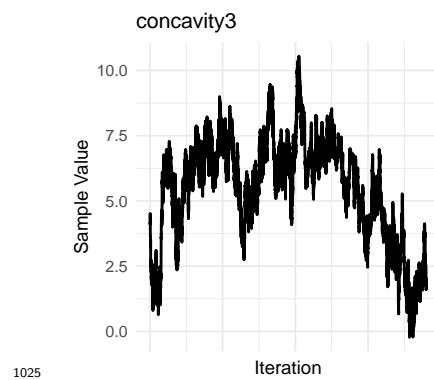
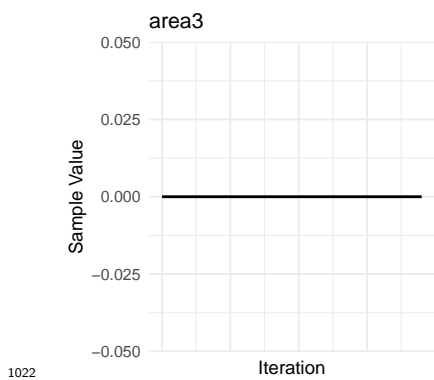
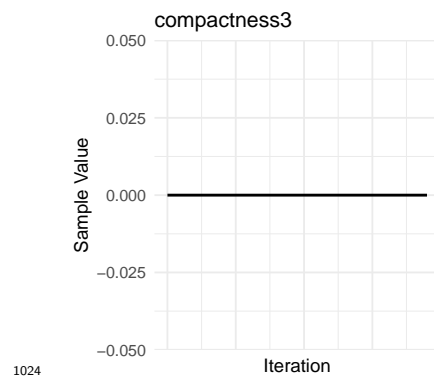
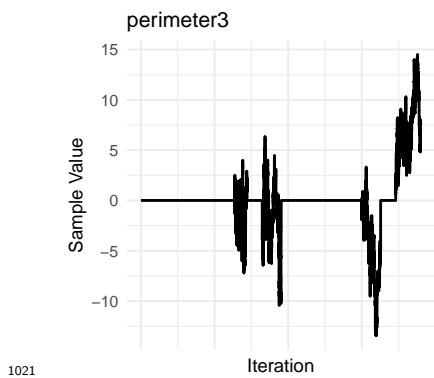
999

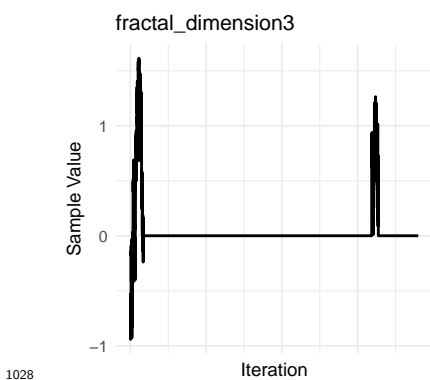
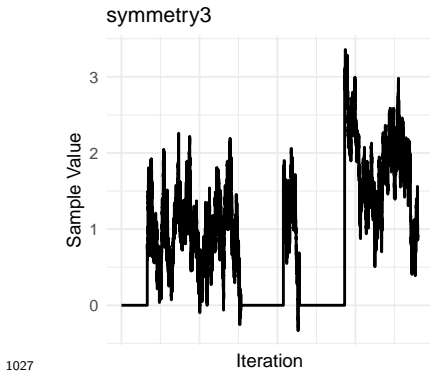
1002











1029 Variables with posterior inclusion probabil-
1030 ity set to zero, like `fractal_dimension1`, have no
1031 exploration in their traceplot at all.

1032 The effective posterior means will be exactly
1033 zero for features with $z_j = 0$ in all samples, and
1034 will be shrunk toward zero for features that
1035 are only sometimes included. This provides au-
1036 tomatic regularization while maintaining inter-
1037 pretability.

1038 Unlike classical methods that select a sin-
1039 gle “best” model, Bayesian variable selection ex-
1040 plores the entire model space and assigns pos-
1041 terior probabilities to each model. The specific
1042 combinations of features the MCMC sampler
1043 visited most frequently can be identified.

1044 Results and Conclusion

1045 The ultimate goal of this analysis is not merely
1046 to build a Bayesian model, but to understand

1047 which cellular characteristics are most indicative
1048 of malignancy. This understanding can inform
1049 clinical decision-making and suggest biological
1050 mechanisms underlying breast cancer.

1051 Coefficient Interpretation

1052 For features with high posterior inclusion prob-
1053 abilities, one interprets the coefficients on the
1054 odds scale. Recall that in logistic regression,
1055 $\exp(\beta_j)$ represents the multiplicative change in
1056 odds of malignancy associated with a one-unit
1057 increase in feature j .

1058 Since features were standardized, a “one-
1059 unit increase” corresponds to a *one standard*
1060 *deviation increase* in the original measure-
1061 ment. This makes coefficients directly compara-
1062 ble across features measured on different scales.

1063 All important features are defined as fea-
1064 tures with posterior inclusion probability greater
1065 than 50%, or features that were included in more
1066 than half of the possible combinations.

```
1067 ##
1068 ## radius1:
1069 ##   Coefficient: -1.6594
1070 ##   Odds ratio: 0.1902
1071 ##   95% CI for OR: (0, 3256.972)
1072 ##   A 1-SD increase in radius1
1073 ## multiplies the odds of
1074 ## malignancy by 0.19
1075 ##
1076 ## texture1:
1077 ##   Coefficient: 2.6739
1078 ##   Odds ratio: 14.4967
1079 ##   95% CI for OR: (4.7125, 45.5557)
1080 ##   A 1-SD increase in texture1
1081 ## multiplies the odds of
1082 ## malignancy by 14.5
1083 ##
1084 ## perimeter1:
1085 ##   Coefficient: -1.5813
1086 ##   Odds ratio: 0.2057
1087 ##   95% CI for OR: (0, 429612.2)
1088 ##   A 1-SD increase in perimeter1
1089 ## multiplies the odds of
1090 ## malignancy by 0.21
1091 ##
```

```

1092 ## area1:
1093 ##   Coefficient: -0.7566
1094 ##   Odds ratio: 0.4692
1095 ##   95% CI for OR: (0, 32938.09)
1096 ##   A 1-SD increase in area1
1097 ##   multiplies the odds of
1098 ##   malignancy by 0.47
1099 ##
1100 ##   smoothness1:
1101 ##   Coefficient: 1.8848
1102 ##   Odds ratio: 6.5848
1103 ##   95% CI for OR: (1.142, 32.7933)
1104 ##   A 1-SD increase in smoothness1
1105 ##   multiplies the odds of
1106 ##   malignancy by 6.58
1107 ##
1108 ##   compactness1:
1109 ##   Coefficient: -3.4053
1110 ##   Odds ratio: 0.0332
1111 ##   95% CI for OR: (0.0013, 1.0583)
1112 ##   A 1-SD increase in compactness1
1113 ##   multiplies the odds of
1114 ##   malignancy by 0.03
1115 ##
1116 ##   radius2:
1117 ##   Coefficient: 1.9384
1118 ##   Odds ratio: 6.9478
1119 ##   95% CI for OR: (0.1581, 1784.535)
1120 ##   A 1-SD increase in radius2
1121 ##   multiplies the odds of
1122 ##   malignancy by 6.95
1123 ##
1124 ##   area2:
1125 ##   Coefficient: 2.494
1126 ##   Odds ratio: 12.11
1127 ##   95% CI for OR: (1, 1231.14)
1128 ##   A 1-SD increase in area2
1129 ##   multiplies the odds of
1130 ##   malignancy by 12.11
1131 ##
1132 ##   smoothness2:
1133 ##   Coefficient: 0.9436
1134 ##   Odds ratio: 2.5692
1135 ##   95% CI for OR: (1, 10.1154)
1136 ##   A 1-SD increase in smoothness2
1137 ##   multiplies the odds of
1138 ##   malignancy by 2.57
1139 ##
1140 ##   concavity2:
1141 ##   Coefficient: -3.4613
1142 ##   Odds ratio: 0.0314
1143 ##   95% CI for OR: (0.002, 0.1925)
1144 ##   A 1-SD increase in concavity2
1145 ##   multiplies the odds of
1146 ##   malignancy by 0.03
1147 ##
1148 ##   concave_points2:
1149 ##   Coefficient: 1.6546
1150 ##   Odds ratio: 5.2311
1151 ##   95% CI for OR: (0.9149, 199.807)
1152 ##   A 1-SD increase in concave_points2
1153 ##   multiplies the odds of
1154 ##   malignancy by 5.23
1155 ##
1156 ##   fractal_dimension2:
1157 ##   Coefficient: -1.4964
1158 ##   Odds ratio: 0.2239
1159 ##   95% CI for OR: (0.0304, 1.3649)
1160 ##   A 1-SD increase in fractal_dimension2
1161 ##   multiplies the odds of
1162 ##   malignancy by 0.22
1163 ##
1164 ##   radius3:
1165 ##   Coefficient: 12.1759
1166 ##   Odds ratio: 194056
1167 ##   95% CI for OR: (3.1018, 639687234)
1168 ##   A 1-SD increase in radius3
1169 ##   multiplies the odds of
1170 ##   malignancy by 194056
1171 ##
1172 ##   concavity3:
1173 ##   Coefficient: 5.4404
1174 ##   Odds ratio: 230.5247
1175 ##   95% CI for OR: (2.9938, 6024.333)
1176 ##   A 1-SD increase in concavity3
1177 ##   multiplies the odds of
1178 ##   malignancy by 230.52
1179 ##
1180 ##   concave_points3:
1181 ##   Coefficient: 2.3546
1182 ##   Odds ratio: 10.534
1183 ##   95% CI for OR: (1, 2045.605)
1184 ##   A 1-SD increase in concave_points3
1185 ##   multiplies the odds of
1186 ##   malignancy by 10.53
1187 ##
1188 ##   symmetry3:
1189 ##   Coefficient: 0.8067
1190 ##   Odds ratio: 2.2405
1191 ##   95% CI for OR: (1, 12.5)

```

30

```
1192 ## A 1-SD increase in symmetry3  
1193 ## multiplies the odds of  
1194 ## malignancy by 2.24
```

1195 Example Interpretation: Consider
1196 **symmetry3**. If there a one stan-
1197 dard deviation increase in the worst
1198 symmetry measurement, the odds
1199 of malignancy multiplies by ap-
1200 proximately $e^{0.8067} \approx 2.24$, holding
1201 all other features constant.

1202 **Ranking the Most Important Features by**
1203 **Inclusion Probability**

1204 While it is known what the important features
1205 are, which of these are the most important?

1206 The following features, as per the above
1207 computations, have a posterior inclusion prob-
1208 ability of 1—they are included in every single
1209 model combination.

- 1210 • The mean measurement of texture
- 1211 • The mean measurement of smoothness
- 1212 • The mean measurement of compactness
- 1213 • The standard error of concavity
- 1214
- 1215 • The worst measurement of radius = The
1216 worst measurement of concavity

1217 **References**

1218 Wolberg, W., Mangasarian, O., and
1219 Street, W. N. (1993). “Breast Can-
1220 cer Wisconsin (Diagnostic).” UCI
1221 Machine Learning Repository. DOI:
1222 <https://doi.org/10.24432/C5DW2B>. 1